Catalysis Today 143 (2009) 120–125

Contents lists available at ScienceDirect

Catalysis Today

journal homepage: www.elsevier.com/locate/cattod

Impact of Al and Ti ions on the dispersion and performance of supported NiMo(W)/SBA-15 catalysts in the HDS and HYD reactions

A. Olivas, T.A. Zepeda *

Centro de Nanociencias y Nanotecnología - UNAM, Km. 107 Carretera Tijuana-Ensenada, CP. 22800, Ensenada, B.C. México, Mexico

ARTICLE INFO

Article history:
Available online 21 October 2008

Keywords:
Hydroprocessing catalysts
NiMo and NiW catalysts
Hydrodesulfurization
Hydrogenation
SBA-15 material
Al and Ti effect
Acidity effect on the dispersion

ABSTRACT

The effect of the aluminum and titanium presence on the catalytic activity of the NiMo/SBA-15 and NiW/SBA-15 catalysts was evaluated in the hydrodesulfurization of dibenzothiophene and biphenyl hydrogenation. The samples were characterized by SP MAS ^{29}Si NMR, S_{BET}, XRD, chemisorption of H_2 and TPD-NH_3. The Ti-containing samples showed higher catalytic performance in both hydroprocessing reactions, in comparison with the Al-containing samples. The presence of Ti ions enhanced the dispersion of the supported active components, and the dispersion of the active species was related to the acidity of the supports. Finally, the W based catalysts showed higher activity in the hydroprocessing reactions than the traditional Mo based catalysts.

1. Introduction

Today the environmental regulations on the sulfur and aromatics content of diesel fuels are leading refiners to develop novel catalysts for the production of ultra-low sulfur diesel. In consideration of this for 2009 the sulfur contents from diesel fractions need to be lower than 10 ppm and the cetane number higher than 51 [1–3]. The molybdenum-based hydroprocessing catalysts promoted by Co and Ni are usually supported on γ-Al_2O_3 [4]. Unfortunately these catalysts in the hydroprocessing of the heavy petroleum fractions, especially in the Maya-Mexico oil type complex fractions, are not effective enough to satisfy the new environmental legislation. The need to produce clean engine fuel combined with the prospect of processing poor-quality feedstock petroleum, has stimulated the interest in the synthesis of novel effective catalysts for deep hydroprocessing of diesel and gas–oil [5,6].

Current strategies for the design of novel HDS catalysts often include variations in the preparation method, active phase formulation and the variation or modification of the support [7]. Many new materials have been chosen as support for the preparation of Mo(W) active component and Co or Ni promoters [7]. For this reason, the use of mesoporous silicate materials such as HMS, MCM-41 and SBA-15, which have large pore diameters and higher surface areas than the Al_2O_3 [7–9], have attracted widespread attention as new potential materials for the preparation of novel supported hydrotreating catalysts [7–10]. Several reports have been made to develop high performance hydrotreating catalysts supported on heteroatoms-containing (Ti, Al, Zr, etc.) mesoporous silicate materials [11–13]. In particular, the Al and Ti-containing SBA-15 material has thicker pore walls and acceptable hydrothermal stability [12]. This is an important characteristic for the preparation of hydrotreating catalysts. Important works have been reported on the potential of the SBA-15 material by the preparation of hydroprocessing catalysts. Vradman et al. [14] reported the excellent performance of NiW/SBA-15 catalyst in the deep hydrodesulfurization (HDS) of petroleum feedstock's. Murali Dhar et al. [15] studied the hydrodesulfurization of thiophene (TP) over Mo, CoMo and NiMo catalysts supported on SBA-15 material. The authors reported higher activities of the all supported-SBA-15-catalysts compared with a traditional alumina-supported catalyst, and the superior activity was observed in the CoMo catalysts. Sampieri et al. [16] studied the effect of Mo loading supported on SBA-15 and MCM-41 materials. The authors observed superior performance on the overall HDS of dibenzothiophene (DBT) in the SBA-15 supported catalysts in comparison with MCM-41 supported ones. Nava et al. [12] studied the effect of Ti-loading CoMo/SBA-15 catalysts on the overall activity in the HDS of DBT. The authors reported that the Ti-containing catalysts were more active than the Ti-free counterpart and traditional alumina-supported catalyst. Recently Murali Dhar et al. reported the effect of Al [17] and Zr [18] loading on the HDS of TP and hydrogenation (HYD) of

---

* Corresponding author. Tel.: +52 6461744602; fax: +52 6461744603.
E-mail address: trino@icp.csic.es (T.A. Zepeda).

0920-5861/$ – see front matter © 2008 Elsevier B.V. All rights reserved.
doi:10.1016/j.cattod.2008.09.001

cyclohexene (CH) over of Mo, CoMo and NiMo catalysts supported on SBA-15 material. The Zr-loading catalyst manifested superior activity in HDS of TP, while the Al-loading catalyst was more active in the HYD of CH, and these samples were more active than traditional alumina-supported catalyst. Superior activity in both HDS and HYD reactions was observed over NiMo catalysts, in comparison with Mo and CoMo catalysts. Probably the use of heteroatoms-containing SBA-15 materials could be a candidate for newer more active and effective supported hydrotreating catalysts than the typical industrial supported Co(Ni)Mo/γ-Al_2O_3. In this work we report the effect of Al and Ti-load on the catalytic activity of NiMo/SBA-15 and NiW/SBA-15 catalysts in the HYD of biphenyl (BP) and the HDS of DBT. The samples were characterized by SP MAS ^{29}Si NMR, S_{BET}, XRD, chemisorption of H_2 and TPD-NH_3.

2. Experimental

2.1. Synthesis of supports and catalysts

The SBA-15, Al-SBA-15 and Ti-SBA-15 supports (with an atomic ratio of Si/Al(Ti) = 40) were synthesized by following a similar procedure to that described by Zhao et al. [19] and Yue et al. [20]. The incorporation of Al and Ti ions into the mesostructure SBA-15 was carried out by the direct-synthesis method using aluminum isopropoxide (98%, Aldrich) and titanium butoxide (97%, Aldrich) as the Al and Ti source following the published procedure [20]. The solid product obtained was filtered, dried at room temperature for 24 h and then at 393 K for 3 h, and finally calcined in air at 773 K for 6 h with a heating rate of 1 °C/min.

The catalysts were prepared by simultaneous impregnation method using the pore filling method source following the published procedure [9]. The samples were prepared with the same atomic loading of the Mo and W elements, taking into account the difference of the atomic weight between these atoms. The loading of the Mo(W) and Ni species were determinate by ICP and they are reported in Table 1.

2.2. Characterization methods

The samples were characterized by solid-state single pulse (SP) mass atomic spectra (MAS) nuclear magnetic resonance (^{29}Si NMR) measurements, the textural properties of the supports and catalysts, the X-ray patterns, the metal dispersion and acidity of the pure supports. The experimental details are reported elsewhere [21–22].

2.3. Catalytic activity measurements

Before of the reaction, the catalysts were activated by sulfidation performed in a U-shaped glass flow reactor. First, the sample was flushed in a nitrogen flow, gradually increasing the temperature to 423 K and then switching to the sulfidation mixture (H_2/H_2S 10 vol.% H_2S) at a flow of 60 mL min^{-1} and increasing the temperature to 673 K, reaching this temperature within 2.5 h and maintaining this temperature for 2 h.

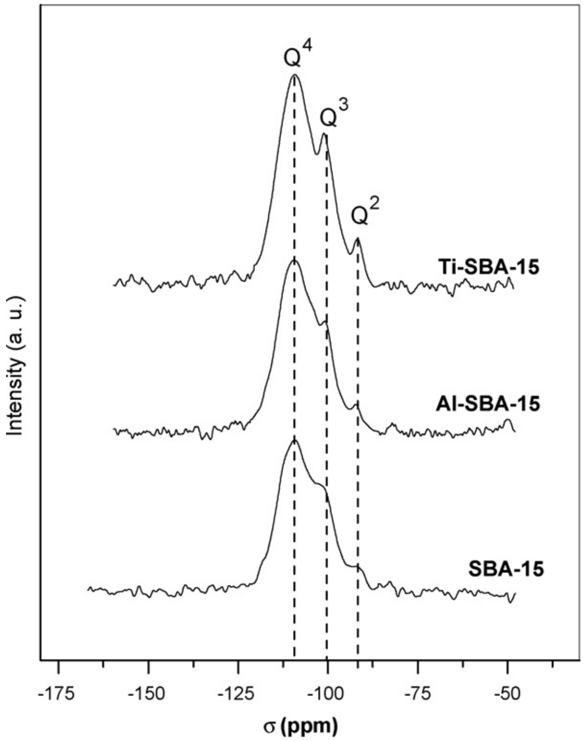

Fig. 1. ^{29}Si-Nuclear magnetic resonance spectra of the pure supports.

The catalytic activity in the reaction of HYD of BP and HDS of DBT were measured in a batch Parr reactor. The experimental details are reported elsewhere [13].

3. Results and discussion

The ^{29}Si NMR spectra of the calcined SBA-15, Al-SBA-15 and Ti-SBA-15 supports are shown in Fig. 1. All spectra showed three peaks observed close to −92, −100 and at −110 ppm. The peak center at −92 ppm corresponds to the resonance associated with Q^2 species and the peaks at −100 and −110 were assigned to the resonances corresponds to the Q^3 and Q^4 species, respectively [23]. The Q^4, Q^3 and Q^2 resonances are assigned to $Si(OSi)_4$, $Si(OSi)_3OH$ and $Si(OSi)_2(OH)_2$ species, respectively [23,24]. In previous report [22] it was compared the ^{29}Si NMR spectra of Ti ions containing varying the Ti content into HMS framework (the samples were

Table 1
Metal composition and Textural properties of the supports and catalysts and H_2-chemisorption data of the catalysts.

Samples	Mo[a] (mmol $g_{support}^{-1}$)	W[a] (mmol $g_{support}^{-1}$)	Ni[a] (mmol $g_{support}^{-1}$)	S_{BET} (m^2/g)	APD (nm)	APV (cm^3/g)	H_2 uptake[b] (μmol g^{-1})
SBA-15	–	–	–	1167	5.6	1.91	–
Al-SBA-15	–	–	–	1083	5.5	1.87	–
Ti-SBA-15	–	–	–	971	5.4	1.74	–
NiMo/SBA-15	0.98	–	0.53	598	5.2	1.18	69.3
NiMo/Al-SBA-15	1.02	–	0.54	698	5.3	1.29	78.2
NiMo/Ti-SBA-15	0.99	–	0.54	672	5.3	1.11	84.3
NiW/SBA-15	–	0.97	0.53	515	4.0	1.32	75.3
NiW/Al-SBA-15	–	1.02	0.52	621	4.1	1.09	87.1
NiW/Ti-SBA-15	–	0.98	0.53	587	4.7	0.97	92.2

[a] Determined by ICP.
[b] Chemisorption capacity as determined by pulse method of H_2 chemisorption in the oxidized catalysts.

prepared with a Si/Ti molar ratio equal to that of our samples). A dramatic increment in the amount of Q^4, Q^3 and Q^2 species was observed in all Ti-containing samples. This observation was attributed to the formation of a cross-linked framework by the presence of Ti ions. Therefore, we could expect in our samples higher values of Q^4, Q^3 and Q^2 in the Al and Ti-containing samples than those for the SBA-15 sample, and indeed this happened. This broadening could be attributed to the effect of the heteroatom sites on the chemical environment of the adjacent Si atoms. Indeed, the amount of Q^4, Q^3 and Q^2 species are incremented strongly in the presence of Al and Ti ions, but the increment of the Q^2 resonance intensity was higher than the Q^3 value, and the increment of the intensity of both, Q^2 and Q^3, was higher than the increment of the Q^4 resonance intensity. Comparing the ^{29}Si NMR spectra of the pure SBA-15 sample with the Al and Ti-containing SBA-15 samples, we can note that the increment on the intensities of Q^4, Q^3 and Q^2 resonances is higher in the Ti-containing sample than those of the Al-SBA-15 sample. In agreement with previous report [22], we could take the $Q^4/(Q^2 + Q^3)$ intensity ratio to have an idea on the incorporation of Al and Ti ions into the silica framework. As it was expected, this ratio is lower in the Al and Ti-containing samples in comparison with the pure SBA-15 sample, but the lowest ratio was observed in the Ti-containing sample. Then we could conclude that the Al and Ti ions were incorporated into of SBA-15 material due to the modification in the chemical environment of the adjacent Si. Also, a higher effect of Ti ion incorporation was observed as compared to the effect of Al ion incorporation.

The nitrogen adsorption isotherms of the pure supports and catalysts (data not shown here) were of type IV isotherms, according to the IUPAC classification [25]. All samples showed an appreciable type H1 hysteresis loops indicating the presence of textural mesopores and cylindrical pores [26]. The textural properties, such as surface area (S_{BET}), average pore diameter (APD) and average pore volume (APV) are summarized in Table 1. In this table, we can note that the pure SBA-15 support shows the highest specific area (1167 $m^2 g^{-1}$). The specific area of the supports follows the order: SBA-15 > Al-SBA-15 > Ti-SBA-15. This means that the introduction of Al or Ti ions into the SBA-15 material modifies the specific area. Also, both APD and APV decreases in the presence of heteroatoms-containing, the last order is also valid for these two parameters.

The S_{BET} specific area of the supports decreased upon incorporation of the NiMo or NiW phases (Table 1). Independently of the Al and Ti content, we can note higher surface area values in the NiMo samples in comparison with the NiW samples. The S_{BET} values of supported NiMo catalysts follow the order: NiMo/SBA-15 < NiMo/Ti-SBA-15 < NiMo/Al-SBA-15, this same order is also valid for the NiW samples. Analyzing the S_{BET} values of the pure supports with the homologous catalysts, we can observe that the largest decrement of the S_{BET} value was observed in both, Al and Ti-free samples, while the lowest decrement in the S_{BET} value was observed in both Ti-containing samples. Also this observation is valid for the APD values, but in the NiMo samples the lowest decrement in the APD was observed (0.1–0.4 nm vs. 0.7–1.6 nm, respect to the APD of the pure supports). Contrary to the S_{BET} and APD values, the APV values do not follow a clear tendency, but in general the APV values decreases after upon incorporation of the NiMo or NiW phases.

The X-ray patterns recorded in the range 5–60° in 2θ of the supported NiMo and NiW catalysts are shown in Fig. 2. The wide-angle X-ray patterns of all the samples exhibited a broad line between 15° and 35°, which was attributed to the siliceous amorphous phase [11–13]. All NiMo samples show an intense reflection peak at 22.7° 2θ overlapping with the broad diffraction peaks of the amorphous part of the support, which is characteristic at crystalline of MoO_3 phase (JCPDS card 1-076-1003). An additional intense reflection peak at 25.6° 2θ was observed in the NiMo/SBA-15 sample and this reflection is attributed to the presence of the β-$NiMoO_4$ phase (JCPDS card 21-0868). One can note that the intensities of the reflections observed in the NiMo/SBA-15 sample are higher in comparison with both, Al and Ti-containing NiMo samples. The absence of the reflection characteristic to the β-$NiMoO_4$ phase in both, the Al and Ti-containing NiMo samples, could indicate that the presence of Ti and Al ions inhibit the formation of this phase, and it is difficult to sulfide under the conditions employed in this work. Contrary to the NiMo samples, the NiW samples showed a small reflection peak at 23.5° 2θ associated with the presence of WO_3 phase. Newly, we can note that the free-heteroatoms sample (NiW/SBA-15) exhibits the more intense reflection peak, in comparison with the Al and Ti-containing samples. Also, in general we can note that the intensities of the reflections are higher in the NiMo samples than that in the NiW samples. We could conclude that the presence of Al and Ti ions enhances the dispersion of the supported species, and superior dispersion of the active components could be in the NiW samples, in comparison with the NiMo samples. This was corroborated by H_2-chemisorption data. The H_2-chemisorption data of the catalysts are shown in Table 1. We can note superior H_2-chemisorption in the

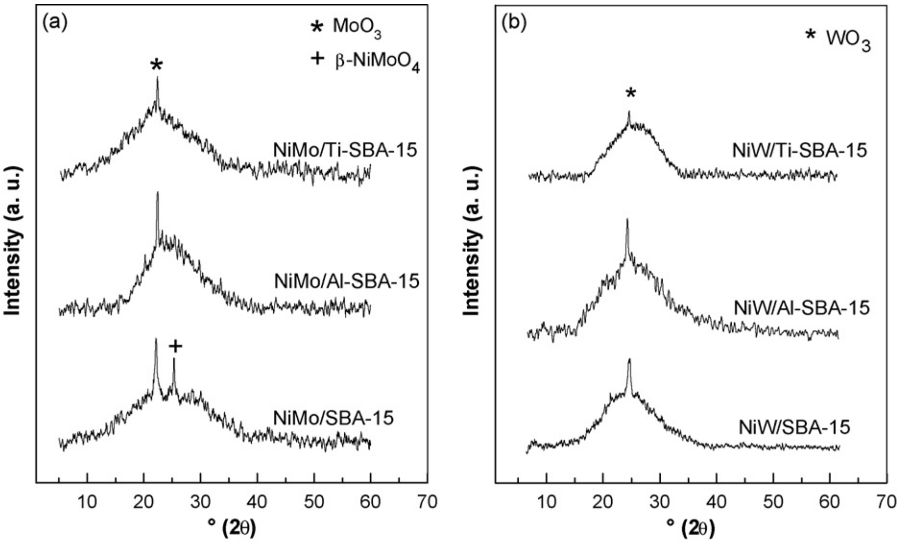

Fig. 2. X-ray patterns correspond to the supported NiMo catalysts (a) and supported NiW catalysts (b).

NiW based samples in comparison with the NiMo samples, in agreement with DRX results. Also, independently of the phase type (NiMo or NiW), we can note lower H_2-chemisorption in the free-heteroatoms samples (NiMo/SBA-15 and NiW/SBA-15) and higher H_2-chemisorption in the Ti-containing samples (NiMo/Ti-SBA-15 and NiW/Ti-SBA-15). Our results could indicate that the presence of Ti ions into of SBA-15 sample enhances the dispersion of the supported transition metals. These results are opposed to our previous study on the dispersion of transition metals supported on Al and Ti-containing HMS system [13]. This could be related to the structure type of the substrate (HMS and SBA-15) and the formation the different surface Al and Ti species on the different substrates. With our results we cannot explain this point, but more experiments are necessary to clarify this question.

The TPD-NH_3 profiles of the pure supports are shown in Fig. 3. The concentrations after fitting of the experimental curves to sum of Gaussian lines of the weak ($T < 500$ K), medium ($500\ \text{K} < T < 700$ K) and strong ($T > 700$ K) strength acid sites, expressed as mmole of NH_3 desorbed are summarized in Table 2. The total acidity of the samples was calculated as the sum of the weak, medium and strong acid sites. One can note that the SBA-15 support shows weak and medium acid sites with the main contribution of weak type. The Al and Ti-containing SBA-15 supports show the presence of weak, medium and strong acid sites, with the main contribution of medium type. We can note that the Ti-containing sample has higher acidity medium type, while acidity strong type is similar to the Al-containing sample, but both medium and strong acidity sites contribute on the total acidity. The higher total acidity was observed in the Ti-containing sample, in comparison with the other samples. In agreement with Del Arco et al. [27], the medium and strong acidity could be associated with the presence of Brønsted acidity sites. Then in agreement with the last author and with our previous report [21], the presence of Al and Ti ions into of SBA-15 material enhances the population of Brønsted acidity sites. We found a tendency between the supports acidity and the dispersion of the supported species; this tendency is shown in Fig. 4. Then, it is possible to conclude that the dispersion of the transition metals in SBA-15 system depends strongly on the substrate acidity, and specifically the dispersion of the supported metals could be involved with the medium and strong acidity sites, this in agreement with Del Arco et al. [27].

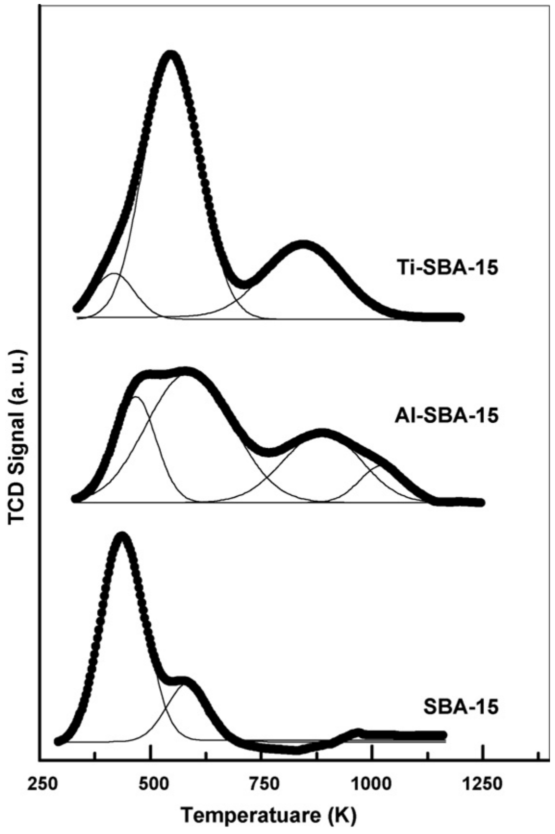

Fig. 3. TPD-NH_3 profiles and the Gaussian deconvolution lines of the calcined samples.

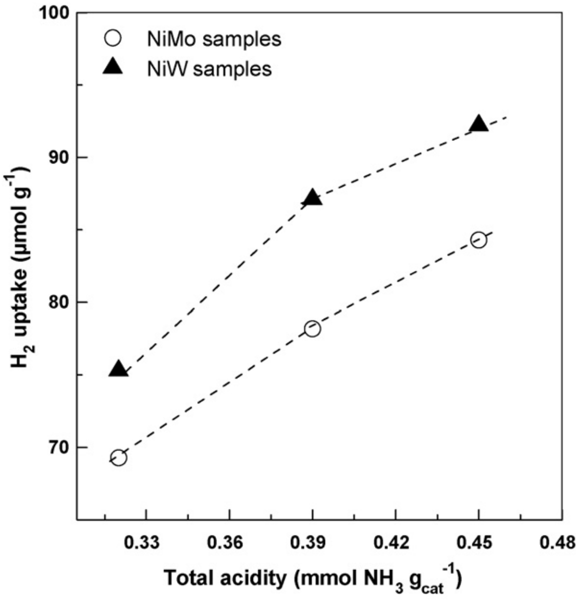

Fig. 4. Correlation between the acidity of the pure supports with the dispersion of the supported species.

We tested the samples in both reactions, HYD of BP and HDS of DBT in batch reactor. The HYD and HDS reactions were carried out under the same reaction conditions. The rate constants normalized by surface area for these two reactions are shown in Table 3. The product distributions to 50% of conversion by the HYD of BP and HDS of DBT are shown in Figs. 5 and 6, respectively. The reaction products by the HYD of BP were dicyclohexyl (DCH) and cyclohexylbencene (CHB), while the tetra-hydro-dibenzothio-

Table 2
TPD-NH_3 acidity of the pure supports.

Sample	Strength of acid sites[a] (mmol NH_3 g_{cat}^{-1})			
	Weak <500 K	Medium 500–700 K	Strong >700 K	Total
SBA-15	0.25	0.07	–	0.32
Al-SBA-15	0.10	0.18	0.11	0.39
Ti-SBA-15	0.05	0.30	0.10	0.45

[a] Calculated from amount of desorbed NH_3 by TPD profiles.

Table 3
Rate constants for the HYD[a] of BP and HDS[a] of DBT.

Samples	$\kappa_{(HYD)} \times 10^9$ [$mol_{DBT}\ s^{-1}\ m^{-2}$]	$\kappa_{(HDS)} \times 10^9$ [$mol_{DBT}\ s^{-1}\ m^{-2}$]
NiMo/SBA-15	7.8	2.2
NiMo/Al-SBA-15	8.4	3.3
NiMo/Ti-SBA-15	9.2	4.1
NiW/SBA-15	8.1	3.8
NiW/Al-SBA-15	10.6	5.7
NiW/Ti-SBA-15	13.8	7.7
NiW/γ-Al_2O_3	20.4	9.2

[a] In batch reactor carried out for 8 h at 598 K under hydrogen pressure of 5.5 MPa.

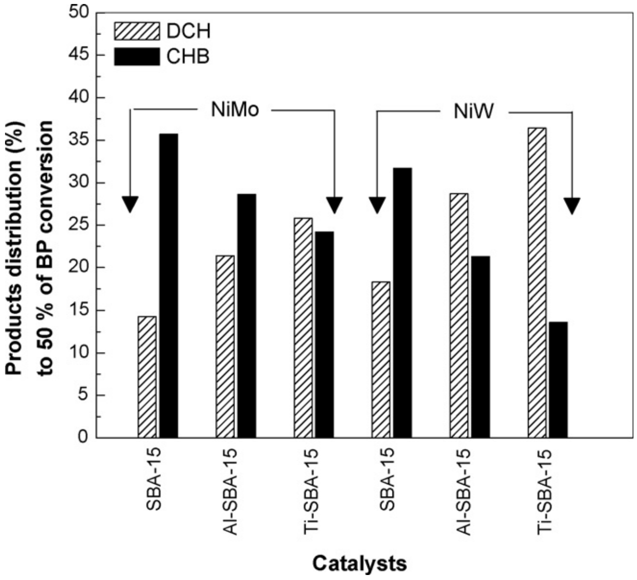

Fig. 5. Products distribution by the HYD of BP to 50% of conversion.

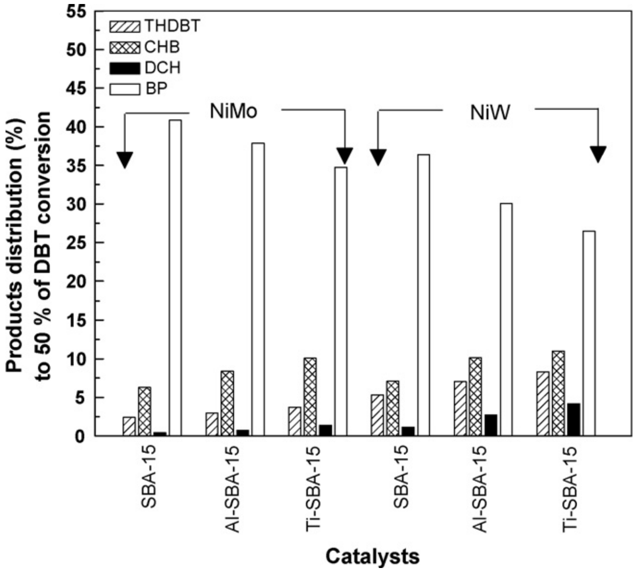

Fig. 6. Products distribution by the HDS of DBT to 50% of conversion.

phene (THDBT), biphenyl, DCH and CHB were the reactions products by the HDS of DBT. We could take the DCH/CHB and (THDBT + DCH + CHB)/BP ratios as measurements of the hydrogenation ability for the HYD and HDS, respectively. The NiW samples showed higher hydrogenation ability in both, HYD and HDS reactions, in comparison with the NiMo samples, but the predominant reaction pathway for the HDS of DBT, in all samples, was via direct desulfurization. Also, independently of the reaction and the active phase (NiMo or NiW), the Ti-containing samples showed superior hydrogenation ability, while the heteroatoms-free samples showed the lower hydrogenation ability. Then, we could conclude that the Ti and Al ions enhance the hydrogenation ability of the samples, but the higher hydrogenation performance is in the presence of Ti ions. Independently of the reaction (HDS or HYD), the hydrogenation ability of the samples could be associated with the acidity properties [27,28]. An interesting correlation between the total acidity of the samples with the hydrogenation ability in both HYD and HDS reactions is shown in Fig. 7(a) and (b), respectively. Analyzing these figures we could assume that the ring saturation ability could be related to the acidity of the samples. The W loaded samples showed higher saturation ability of the ring molecules [27]. This observation is consistent that the active W sites are characterized for having a strong acid, and this was observed with our measures of the acidity [27,28]. Also in agreement with our previous reports [29] the acidity of the samples could be related to the ability by the heterolitic hydrogen dissociation, involving the hydrogen dissociated in the ring saturation of the samples [29]. Then, we could conclude that the acidity of the samples has a strong effect on the hydrogenation ability of the samples.

Finally, we found that the catalytic performance, in both reactions, is related to the dispersion of the active components. Fig. 8 shows a correlation between the dispersion of the supported metals (for H_2-chemisorption data) with the catalytic activity in both, HYD and HDS reactions. Then, in agreement with our results and with our previous reports [11,13,22], we could conclude that the dispersion of the active components has a strong effect on the response of the catalysts in the tested reactions.

Analyzing the rate constants shown in Table 3, again we can note that, independently of the reaction, the NiW samples showed higher catalytic performance, in comparison with the NiMo samples. Newly, the Ti-containing samples showed superior catalytic activity in comparison with the other samples. In general, the hydrogenation activity was approximately 2.6 times more active than the hydrodesulfurization activity, this could be related to the formation of H_2S during the HDS reaction, and the presence of this gas could be inhibiting the active sites [21]. For comparison, in Table 3, we included the reactions constant (normalized by

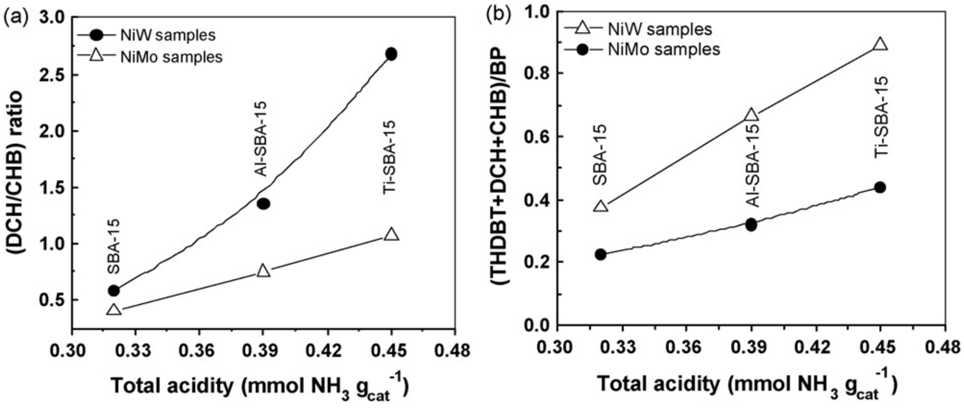

Fig. 7. Correlation between the acidity of the samples with the catalytic hydrogenation ability in both, HYD of BP (a) and HDS of DBT (b) reactions.

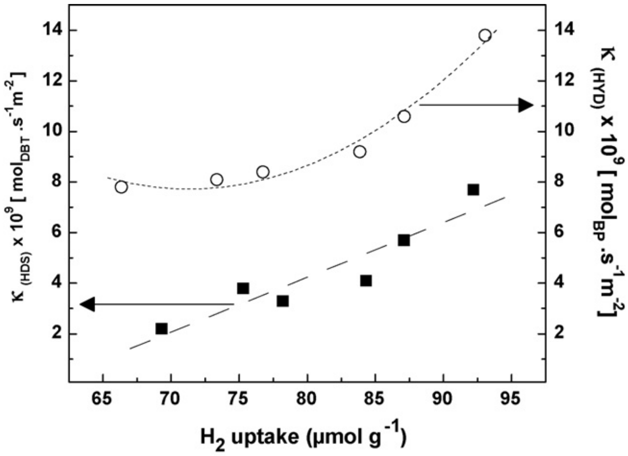

Fig. 8. Correlation between the dispersion of the supported metals (H_2-chemisorption data) with the catalytic activity in both, HYD of BP and HDS of DBT reactions.

surface area) for the HYD and HDS reactions over the reference NiW/γ-Al_2O_3 sample, test under same reaction conditions. Comparing our reaction rate constants normalized by surface area with those of the reference sample, we could note superior performance for the reference sample. Nevertheless, is valid to assume that we could optimize the load of the active components to that of our samples having between 2.5 and 3 times more surface area than that of the reference one, and obtain supported NiMo or NiW catalysts on the mesoporous SBA-15 material with superior catalytic performance than the reference one.

4. Conclusions

The introduction of Ti ions into the framework of the SBA-15 material results in complete incorporation in comparison with the Al ions. Incorporation of Al and Ti ions leads to significant changes in the catalytic properties of the catalysts in both, HYD and HDS reactions enhance the hydrogenation ability of the samples, and this hydrogenation ability was related to the acidity of the samples. Superior performance and hydrogenation ability were observed on the Ti and W content samples. Finally, the catalytic performance of the samples was related to the dispersion of the supported metals, and the dispersion of the supported metals was related to the acidity properties of the supports.

Acknowledgements

T.A. Zepeda is grateful to CNyN-UNAM México for financial support. The authors are grateful to Eric Flores and Eloisa Aparicio for the valuable technical assistance.

References

[1] D. Eastwood, H. Van de Venne, NPRA Annual Meeting, San Antonio, TX, March, 1990.
[2] K.G. Knudsen, B.H. Cooper, H. Topsøe, Appl. Catal. A Gen. 189 (1999) 205.
[3] D.D. Whitehurst, T. Isoda, I. Mochida, Adv. Catal. 42 (1998) 345.
[4] H. Topsoe, B.S. Clausen, F.E. Massoth, Hydrotreating Catalysts: Science and Technology, Springer, Berlin, 1996.
[5] I.V. Babich, J.A. Moulijn, Fuel 82 (2003) 607.
[6] V. Sundaramurthy, A.K. Dalai, J. Adjaye, J. Mol. Catal. A: Chem 294 (2008) 20.
[7] D. Trong On, D. Desplantier-Giscard, C. Danumah, S. Kaliaguine, Appl. Catal. A: Gen. 253 (2003) 545.
[8] G. Murali Dhar, B.N. Srinivas, M.S. Rana, M. Kumar, S.K. Maity, Catal. Today 86 (2003) 45.
[9] B. Pawelec, P. Castaño, T.A. Zepeda, Appl. Surf. Sci. 254 (13) (2008) 4092.
[10] Carlos F. Linares, Patricia Amézqueta and Carlos Scott, Fuel 87 (2008) 2817.
[11] T.A. Zepeda, B. Pawelec, A. Olivas, J.L.G. Fierro, Mater. Res. Innov. 11 (1) (2007) 54.
[12] R. Nava, R.A. Ortega, G. Alonso, C. Ornelas, B. Pawelec, J.L.G. Fierro, Catal. Today 127 (2007) 70.
[13] T.A. Zepeda, B. Pawelec, J.L.G. Fierro, A. Olivas, S. Fuentes, T. Halachev, Microp. Mesop. Mat. 111 (1–3) (2008) 157.
[14] L. Vradman, M.V. Landau, M. Herskowitz, V. Ezersky, M. Talianker, S. Nikitenko, Y. Koltypin, A. Gedanken, J. Catal. 213 (2003) 163.
[15] G. Murali Dhar, G. Muthu Kumaran, Kumar Manoj, K.S. Rawat, L.D. Sharma, B. David Raju, K.S. Rama Rao, Catal. Today 99 (2005) 309.
[16] A. Sampieri, S. Pronier, J. Blanchard, M. Breysse, S. Brunet, K. Fajerwerg, C. Louis, G. Pérot, Catal. Today 107/108 (2005) 537.
[17] G. Muthu Kumaran, S. Garg, K. Soni, M. Kumar, L.D. Sharma, G. Murali Dhar, K.S. Rama Rao, Appl. Catal. A: Gen. 305 (2006) 123.
[18] S. Garg, K. Soni, G. Muthu Kumaran, M. Kumar, J.K. Gupta, L.D. Sharma, G. Murali Dhar, Catal. Today 130 (2008) 302.
[19] D. Zhao, Q. Huo, J. Fend, B.F. Chmelka, G.D. Stucky, J. Am. Chem. Soc. 120 (1998) 6024.
[20] Y. Yue, A. Gedeon, J. Bonardt, J. Espinose, N. Melosh, J. Fraissard, Chem. Commun. 19 (1999) 1967.
[21] T.A. Zepeda, B. Pawelec, J.L.G. Fierro, T. Halachev, Appl. Catal. B: Environ. 71 (2007) 223.
[22] T.A. Zepeda, J.L.G. Fierro, B. Pawelec, R. Nava, T. Klimova, G.A. Fuentes, T. Halachev, Chem. Mater. 17 (2005) 4062.
[23] M.L. Schraml-Marth, K. Waltehr, A. Wokaun, J. Non-Cryst. Solids 111 (1992) 143.
[24] W. Zhang, M. Fröba, J. Wang, P.T. Tanev, J. Wong, T.J. Pinnavaia, J. Am. Chem. Soc. 118 (1996) 9164.
[25] A.Y. Khodakov, A. Griboval-Constant, R. Bechara, F.J. Villain, Phys. Chem. B 105 (2001) 9805.
[26] R. Mokaia, W.J. Jones, J. Catal. 172 (1997) 211.
[27] M. Del Arco, S.R.G. Carrazan, C. Martin, I. Martin, V. Rives, Spectrochim. Acta 50 (1994) 697.
[28] S. Lecarpentier, J. van Gestel, K. Thomas, J. Gilson, M. Houalla, J. Catal. 254 (2008) 49.
[29] T.A. Zepeda, B. Pawelec, J.L.G. Fierro, T. Halachev, J. Catal. 242 (2006) 254.